Unexpected Multi-Step Transformation of AgCuS to AgAuS During Nanoparticle Cation Exchange

Sarah K. O'Boyle, 1 Katelyn J. Baumler, 1 and Raymond E. Schaak 1,2,3,*

E-mail: res20@psu.edu

ABSTRACT

Cation exchange reactions can modify the compositions of colloidal nanoparticles, providing easy access to compounds and/or nanoparticles that may not be accessible directly. The most common nanoparticle cation exchange reactions replace monovalent cations with divalent cations or vice versa, but some monovalent-to-monovalent exchanges have been reported. Here, we dissect the reaction of as-synthesized AgCuS nanocrystals with Au⁺ to form AgAuS, initially hypothesizing that Au⁺ could be selective for Cu⁺ (rather than for Ag⁺) based on a known Au⁺-for-Cu⁺ exchange and the stability of the targeted AgAuS product. Unexpectedly, we find this system and the putative cation exchange reaction to be much more complex than anticipated. First, the starting AgCuS nanoparticles, which match literature reports, are more accurately described as a hybrid of Ag and a variant of AgCuS that is structurally related to mckinstryite Ag₅Cu₃S₄. Second, the initial reaction of Aq-AqCuS with Au⁺ results in galvanic replacement to transform the Aq component to an Au_vAg_{1-v} alloy. Third, continued reaction with Au⁺ initiates cation exchange with Cu⁺ in Au_vAg_{1-v}-AgCuS to form Au_vAg_{1-v}-Ag₃Cu_xAu_{1-x}S₂ and then Au_vAg_{1-v}-AgAuS, which is the final product. Crystal structure relationships among mckinstryite-type AgCuS, Ag₃Cu_xAu_{1-x}S₂, and AgAuS help to rationalize the transformation pathway. These insights into the reaction of "AgCuS" with Au⁺ reveal the potential complexity of seemingly simple nanoparticle reactions and highlight the importance of thorough compositional, structural, and morphological characterization before, during, and after such reactions.

¹ Department of Chemistry, ² Department of Chemical Engineering, and ³ Materials Research Institute, The Pennsylvania State University, University Park, PA 16802, United States.

INTRODUCTION

Cation exchange reactions of metal chalcogenide nanoparticles provide a powerful platform for synthesizing products having compositions, crystal structures, and morphologies that are not otherwise accessible. 1-9 These reactions rely on a chemical driving force, such as coordination by solvents or solvated ligands, that draws the cation in the starting metal chalcogenide out of the nanocrystal while replacing it with another cation to form a new phase that retains the morphology and, often, the anion structure. Most cation exchange reactions of metal chalcogenide nanoparticles begin with single-metal templates, such as copper sulfide, where only one type of cation is available for exchange. 4,9-15 Such starting nanoparticles provide access to diverse products. For example, copper sulfide nanoparticles can undergo complete exchange with other metal cations to form products such as ZnS and CdS or partial exchange to form mixed-metal compounds such as CuInS₂ or phase-segregated heterostructures such as ZnS-CdS Janus particles. 1,8,16,17 Cation exchange reactions applied to multicomponent heterostructured nanoparticles, such as ZnS-CdS, can sometimes be selective for one metal versus another. For example, when a Cu⁺ exchange was carried out on ZnS-CdS and MnS-ZnS heterostructured nanorods, both produced Cu_{1.8}S–ZnS products, indicating that Cu⁺ exchanged selectively for Cd²⁺ in one case and for Mn²⁺ in the other. 18

As the scope and complexity of nanoparticle cation exchange reactions continues to expand, the application of cation-selective exchange to mixed metal chalcogenides represents an emerging frontier in targeting unique compositions and structures. Mixed metal chalcogenides that have two distinct exchangeable cations provide a useful starting point for understanding how chemistry that has been developed for single-cation templates can be expanded to multi-cation systems. It is especially interesting to consider exchanges in mixed metal chalcogenides that have cations with the same charge but in different crystallographic sites, as these systems could provide a way to probe potential cation-competitive exchange using reaction chemistry that has been established for single-metal systems. In that regard, AgCuS, which contains both Ag⁺ and Cu⁺ cations in distinct sites, is an instructive example as both silver sulfide and copper sulfide, which also contain Ag⁺ and Cu⁺, undergo cation exchange.^{3,4,10,19,20} As a starting point, we focused on Au⁺ as the incoming cation due to literature reports that show Au⁺ exchange can be used on both copper sulfide and silver sulfide to produce gold sulfide. 4,19 We then decided to focus on selectively exchanging Au⁺ with Cu⁺ to form AgAuS based on two other considerations. First, our initial attempts to exchange the Aq⁺ cations in AqCuS with Au⁺ using reaction conditions that had been previously established for the transformation of Ag₂S to Au₂S¹⁹ were unsuccessful, showing only the formation of a AqCI byproduct by XRD. Additionally, both AqCuS and AqAuS have been made as colloidal nanoparticles, 21-24 whereas to our knowledge, Au-Cu-S compounds have not been reported. Therefore, we considered that there would be a high likelihood of transforming AgCuS to AgAuS, rather than to a Au-Cu-S phase, and that this outcome would aid characterization and data interpretation. Given these considerations, we felt that this system represented a relatively simple, straightforward, and plausible exchange to initially target to further develop insights into cation-selective exchange when multiple exchangeable cations are present.

Here, we describe the attempted transformation of as-synthesized AgCuS nanoparticles to AgAuS using cation-selective exchange of Cu⁺ for Au⁺. As discussed above, our expectation was that this reaction would be straightforward. However, we instead discovered very different chemical reactivity, including an unexpected multi-step reaction pathway with processes beyond cation exchange including potential galvanic replacement, internal redistribution of cations, and

redox processes. We provide snapshots that characterize key steps involved in the synthesis of the AgCuS starting nanoparticles, their stoichiometry-dependent reaction with Au⁺, the emergence of Ag and Au domains on the surfaces of the metal sulfide nanoparticles, and the presence of mixed-phase multi-cation intermediates. We also rationalize key aspects of this reaction pathway using crystallographic relationships between the precursors and the products. This crystallographic perspective is important to consider because of the significant difference in ionic radii between Cu⁺ (60 pm) and Au⁺ (137 pm),²⁵ which would be expected to result in a crystal structure rearrangement to accommodate the transformation of AgCuS to AgAuS. In addition to providing unexpected insights into a putative nanoparticle cation exchange reaction, this study highlights the importance of appropriate characterization in understanding key reaction details that are likely to be increasingly important and prominent as the compositional and structural complexity of nanoparticle templates, such as mixed metal chalcogenides, continues to increase.

EXPERIMENTAL SECTION

Chemicals

Copper(I) acetate [97%], silver(I) acetate [99%], gold(III) chloride [AuCl₃, 99%] 1-dodecanethiol [≥98%], oleic acid [90%, technical grade], oleylamine [70%, technical grade], 1-octadecene [90%, technical grade], and trioctylamine [98%] were purchased from Millipore Sigma. All solvents (hexanes, isopropyl alcohol, acetone, and toluene) were of analytical grade. All of the above chemicals were used as received without further purification.

Synthesis of mckinstryite-type AgCuS nanoparticles

We followed a reported procedure for synthesizing AgCuS nanocrystals.²¹ Briefly, 80 mg of copper(I) acetate, 66 mg of silver acetate, 20 mL of trioctylamine, 1.52 mL of oleic acid, and 1.57 mL of oleylamine were combined in a 50 mL 3-neck round bottom flask equipped with a PFTEcoated magnetic stir bar, a reflux condenser, a gas flow adapter, a thermocouple with a glass sheath, and a rubber septum. The set-up was hooked up to a Schlenk manifold through the gas flow adapter and sat in a heating mantle atop a stir plate. The mixture was heated to 150 °C under vacuum and held at that temperature for 30 min while stirring. The mixture was then placed under an inert atmosphere (Ar gas) by cycling between Ar gas and vacuum three times. Then, 2.4 mL of 1-dodecanethiol was injected before the temperature was increased to 230 °C and held there for 2 h while stirring. The mixture was then removed from the heating mantle and allowed to cool to room temperature. The black/brown suspension was transferred and split into two centrifuge tubes and isopropyl alcohol was added before centrifugation. After decanting, the isolated particles were resuspended in toluene, isopropyl alcohol was added, and the particles were centrifuged again. Each centrifugation step was for 2 min at 13,500 rpm. After the second centrifugation, the tubes were decanted, and the particles were suspended in hexanes for storage.

General Au⁺ exchange process

All Au⁺ exchanges follow the same general procedure which is adapted from a published procedure for the conversion of Cu_{2-x}S nanoparticles to Au₂S.⁴ Briefly, 10-20 mg of the presynthesized AgCuS particles (from the preceding section) were dried from solution in a 20 mL septum capped vial. This vial was used as the reaction vessel. Then, 5 mL of octadecene, 2 mL

of oleylamine, and a PFTE coated stir bar were added to the vial open to air and sonicated until completely suspended (~1 min). The vial was then placed on a stir plate. The septum cap was put back on and the vial was placed under bubbling Ar flow in the following manner. A 18G x 3" needle was attached to an Ar gas source via a Schlenk manifold, Ar was turned on, and the needle inserted through the septum and into the mixture. Simultaneously, another 18G x 1 ½" needle was inserted into the septum, so that the needle tip was above the mixture, and attached to a bubbler serving as an outlet for the Ar from the reaction vessel. At this point there was Ar bubbling through the mixture constantly while stirring. In another septum capped vial, AuCl₃ was obtained from a glovebox. The amount of AuCl₃ used was determined by the desired Au:Cu molar ratio; for example, a 1:1 Au:Cu reaction for 10 mg of AgCuS would require 10.7 mg of AuCl₃. Then, 1 mL of an air-free 1:10 toluene:octadecene stock solution was added to the AuCl₃ vial while maintaining the inert atmosphere inside. It was sonicated gently until the solution became a bright yellow and then injected into the reaction vial. It is essential that the toluene/ODE solution has been purged of any air due to the reaction of AuCl₃ with toluene in air which forms an arylgold(III) complex, a viscous black substance, and HCl gas.²⁶ After the addition of the AuCl₃ solution, the mixture was allowed to stir for 20 min at room temperature, during which it turns from a dark brown color to a bright orange-red color; this change is more significant with higher Au:Cu ratios. The mixture was then transferred to a centrifuge tube and isopropyl alcohol was added before centrifuging for 2 min at 13,500 rpm. After decanting, the isolated particles were resuspended in toluene, isopropyl alcohol was added, and the suspension was centrifuged again under the same conditions. After two washes, the isolated particles were resuspended in hexanes for storage.

Characterization Methods

High-angle annular dark field scanning transmission electron microscopy (HAADF-STEM) and scanning transmission electron microscopy coupled with energy dispersive X-ray spectroscopy (STEM-EDS) data were collected on an FEI Talos F200X S/TEM at an accelerating voltage of 200kV. Bruker ESPRIT 2 software was used to analyze and generate HAADF-STEM-EDS elemental maps where pink represents Cu K α , teal represents Ag L α , yellow represents Au L α , and orange represents S K α . ImageJ software was used to analyze TEM images. Powder X-ray diffraction (XRD) data for all materials were collected on a PANalytical Empyrean diffractometer using a Cu K α radiation source.

RESULTS AND DISCUSSION

Several reports describe the synthesis of AgCuS nanoparticles. ^{21,22} We chose one that reported nearly uniform and well dispersed AgCuS nanoparticles using reagents, solvents, ligands, and conditions related to those used to make other cation exchange templates such as copper sulfide. ²¹ Accordingly, AgCuS nanoparticles were synthesized colloidally from Cu(I) acetate and Ag(I) acetate suspended in oleylamine and oleic acid, followed by heating and the addition of 1-dodecanethiol, which serves as the sulfur source. Figure 1 (left) shows powder XRD data for the product of this reaction. Our experimental XRD pattern matches well with the literature report we followed, ²¹ which we find matches more closely with that of mckinstryite Ag₅Cu₃S₄; the rationale, importance, and implications of this assignment will be discussed later. We then reacted the template nanoparticles with AuCl₃ in octadecene, oleylamine, and toluene at room temperature under inert atmosphere. This reaction, which reduced Au³⁺ to Au⁺ *in situ*, has previously been

reported for transforming copper(I) sulfide, Cu_{2-x}S, to gold(I) sulfide, Au₂S, through exchange of Cu⁺ with Au⁺. The powder XRD pattern for the product of this reaction, shown in Figure 1 (right), matches well with petrovskaite AgAuS. The corresponding HAADF-STEM images, along with STEM-EDS element maps for the constituent elements, are shown in Figure 1 as well. Figure 1 also shows EDS spectra that indicate the appearance of Au signal and disappearance of Cu signal after the exchange.

At first glance, the data in Figure 1, coupled with knowledge from the available literature on AgCuS and AqAuS nanoparticles²¹⁻²⁴ and the Au⁺/Cu⁺ cation exchange reaction,⁴ suggest that the cation exchange reaction was successful as planned. It would therefore be tempting to stop here and declare success. However, closer examination of the data for both the AgCuS precursor and the AgAuS product reveal features that suggest that there may be a more complex pathway involved in this reaction than first assumed. Figure 1 shows STEM-EDS element maps for several individual particles of both the AqCuS precursor and the AqAuS product and show that there are deposits of another material on both kinds of particles. The deposits on the AgCuS particles appear to be exclusively Aq, given the strong Aq signal and lack of Cu and S signals in the regions where the deposits are located. In contrast, the deposits on the AgAuS particles appear to be primarily Au. It is well known that materials containing Ag⁺ and Au⁺ are sensitive to reduction by the electron beam during TEM and STEM imaging, and this process can produce similar looking metallic domains as those seen on the particles in Figure 1. We excluded electron beam induced reduction as a factor in these nanoparticle systems because the HAADF-STEM images show minimal change before and after concentrated exposure to the beam during EDS mapping (Figure S1). The minimal change observed is primarily in the starting AgCuS material and involves disappearance (rather than appearance) of some Aq⁰ domains after prolonged exposure to the electron beam; the level to which this occurs is insignificant overall. STEM-EDS analysis of aliquots taken during the synthesis of the AqCuS particles, shown in Figure S2, indicates that Aq⁺ is first reduced, most likely by trioctylamine that is the primary component of the reaction mixture, to metallic Ag nanoparticles in situ early in the reaction. These Ag particles appear to serve as seeds for the formation of the AgCuS phase. This procedure therefore produces multifaceted particles having average diameters of 9-13 nm that consist of a large AgCuS domain attached to a small Ag domain, which is a remnant from the Ag particles that formed in situ prior to formation of AgCuS.

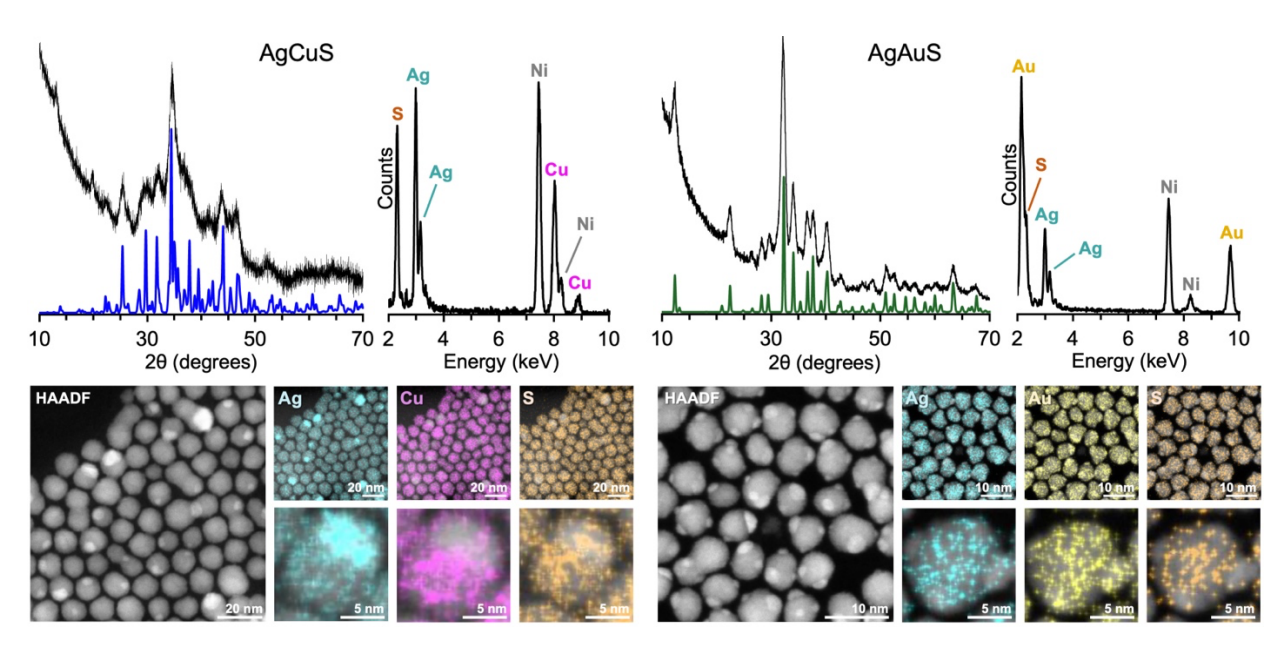


Figure 1. Characterization of (left) as-synthesized AgCuS and (right) the AgAuS product after reaction of AgCuS with Au^+ . Experimental XRD patterns for both materials are shown in black; the mckinstryite $Ag_5Cu_3S_4$ (PDF 00-019-0406) reference pattern (left) is shown in blue and the AgAuS (PDF 04-021-2617) reference pattern (right) is shown in green. For each sample, an EDS spectrum is shown; Ni originates from the Ni TEM grid. Additionally, a HAADF-STEM image is shown for each sample alongside STEM-EDS elemental maps where pink represents Cu Kα, teal represents Ag Lα, yellow represents Au Lα, and orange represents S Kα.

We next evaluated the XRD pattern for the AgCuS particles in greater depth. Figure S4 shows the experimental AgCuS XRD pattern from Figure 1, along with reference patterns for several known Aq-Cu-S phases: α-AqCuS, β-AqCuS (stromeyerite), δ-AqCuS, Aq₅Cu₃S₄ (mckinstryite), and Ag₃CuS₂ (jalpaite). While none of these patterns matches perfectly, we noticed that Ag₅Cu₃S₄ qualitatively matches the experimental pattern, but with observable peak shifts. Specifically and most notably, the peaks at 29.1°, 31.2°, 34.3°, 43.6°, and 46.5° 20 are shifted to higher values of 20 in our experimental pattern. Noting that EDS analysis of the AgCuS particles in Figure 1 showed an approximate 1:1:1 Ag:Cu:S ratio and that some of the Ag was present as Ag nanoparticles, we hypothesized that Aq₅Cu₃S₄ could be Aq deficient; EDS quantification of all samples is provided in Table S1. We therefore simulated a variant of mckinstryite that maintained the same crystal structure but had a composition of AgCuS, which involves a minor decrease in the amount of Ag on some Ag sites relative to Ag₅Cu₃S₄, along with the concomitant addition of Cu to replace these newly defined Ag vacancies. We also decreased the lattice constants from a = 14.047 Å, b = 7.805 Å, and c = 15.691 Å, which are the literature values for mckinstryite, ²⁷ to a = 14.007 Å, b = 7.7752 Å, and c = 15.3662 Å, which empirically match the experimental XRD pattern. Figure 2 shows the experimental XRD pattern for the as-synthesized AgCuS phase, along with mckinstryite-type AqCuS with the slightly compressed unit cell described above; Table S2 shows crystallographic details of mckinstryite and the modified mckinstryite pattern. Additionally, Figure S3 shows how peak overlap makes it difficult to observe metallic Ag nanoparticles with XRD. This simulated pattern matches much better with the experimental data than any of the AgCuS references did, suggesting that the as-synthesized material is better described as AgAgCuS, where the AgCuS has a mckinstryite-type crystal structure that is distinct from the 1:1:1 Ag-Cu-S phases.

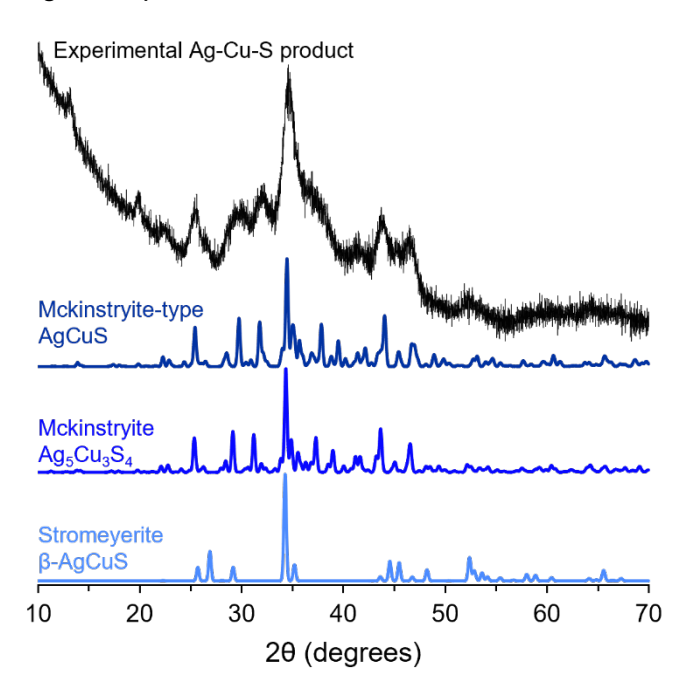


Figure 2. Experimental XRD pattern of as-synthesized AgCuS compared to reference patterns for stromeyerite β-AgCuS (PDF 03-065-2499) and mckinstryite Ag $_5$ Cu $_3$ S $_4$, as well as mckinstryite-type AgCuS, simulated as described in the text.

Now that we have a better understanding of the composition and structure of the as-synthesized nanoparticles, we sought to better understand their reaction with Au⁺ to form AgAuS. We chose to carry out a series of substoichiometric Au⁺ exchanges to mimic the progression of the full cation exchange reaction. We based the stoichiometries of these partial exchange reactions on the amount of Cu present in the initial synthesis used to make the Ag–AgCuS nanoparticles. The substoichiometric Au:Cu ratios we chose were 1:8, 1:5, 1:4, 1:2, 3:4, and 1:1, noting that the original exchange in Figure 1 had a 5:1 ratio of Au:Cu. We then analyzed each of these partial exchanges using STEM-EDS element mapping and XRD.

Figure 3 shows STEM-EDS element maps for each of the substoichiometric Au⁺ exchange reactions applied to the Ag–AgCuS particles. For the 1:8 and 1:5 Au:Cu ratios, which represent the smallest amounts of Au⁺ and mimic the earliest stages of the reaction, the STEM-EDS maps indicate that the Ag domains now contain significant amounts of Au and the Ag signal is less pronounced in these regions. Additionally, the Au signal is not present elsewhere in the particles; it only appears colocalized with Ag in the domains that are attached to the AgCuS particles. Interestingly, while the Ag content decreases in the metal domains attached to the sulfide as Au incorporates, EDS analysis indicates that the overall amount of Ag remains nearly constant. This was determined using the Ag:S ratio as a metric since the sulfur content should remain constant. The initial Ag–AgCuS particles have Ag:S = 1.14 while Ag:S for the 1:8 and 1:5 substoichiometric exchanges are 1.23 and 1.25, respectively; additional EDS quantification are provided in Table S1. Given the experimental error associated with this measurement, the differences among the three values are considered to be insignificant overall. Interestingly, this observation reveals the

presence of an early transformation that occurs prior to the expected cation exchange reaction. We hypothesize the initial introduction of Au^+ to the Ag–AgCuS particles induces a galvanic replacement reaction that reduces Au^{3+} to Au (E° = 1.401 V) while sacrificially oxidizing Ag to Ag^+ (E° = 0.7996 V). The Ag:S ratio was observed to be constant, suggesting that the newly formed Ag^+ incorporates into the AgCuS domain, as will be discussed in detail after analysis of the XRD data.

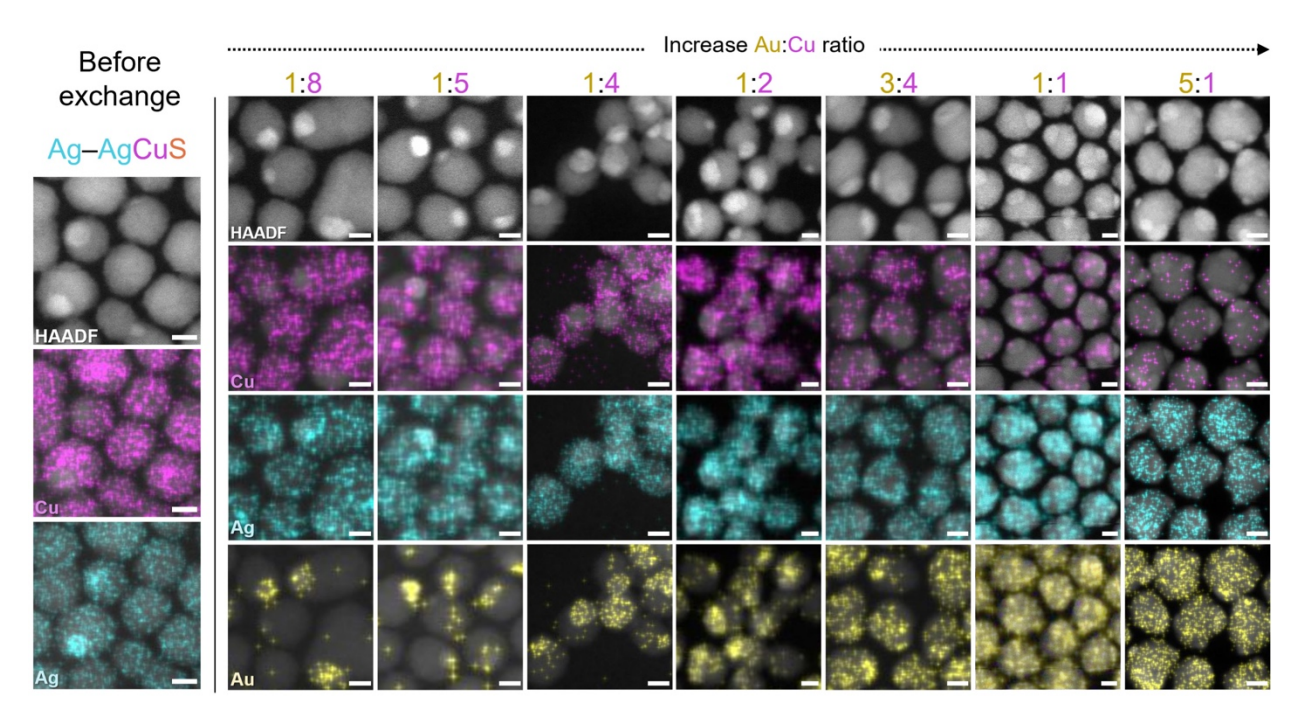


Figure 3. HAADF-STEM images and corresponding overlaid STEM-EDS elemental maps of the starting mckinstryite-type Ag–AgCuS nanoparticles before exchange and samples associated with all Au:Cu ratios. All scale bars are 5 nm. In the STEM-EDS elemental maps, pink represents Cu K α , teal represents Ag L α , and yellow represents Au L α .

For the 1:4 Au:Cu ratio, which mimics the next stage of the reaction beyond the initial incorporation of Au into the Ag region, the Ag signal is almost completely gone from the domain that previously contained Ag and Au, and the Au signal is now dominant in that region (Figure 3). There is also more detectable Au signal in the AgCuS region of the particles, indicating that Au is starting to incorporate into the sulfide domain. Concomitant with the increase in Au signal in the sulfide domain, the Cu signal has decreased. This observation is consistent with the onset of cation exchange. For the 1:2, 3:4, and 1:1 Au:Cu ratios, which represent the final stages of the reaction, the Cu signal continues to progressively decrease until it becomes nearly undetectable. At the same time, the Ag signal remains evenly distributed throughout the particles and consistent in intensity as the Au signal further spreads out across the particles to become colocalized with the Ag. In particular, in the STEM-EDS element maps corresponding to the 3:4, 1:1, and 5:1 Au:Cu ratios, additional regions that correspond only to Au are observed as well, suggesting that Au begins to deposit onto the particles.

Collectively, the STEM-EDS data from the substoichiometric exchanges that track the progress of the reaction paint a picture of a multi-step pathway. First, the Ag domains that form *in situ*

during the synthesis of AgCuS transform to an Au_yAg_{1-y} alloy en route to a domain mostly comprised of Au. This process most likely occurs through galvanic replacement, with Au⁺ depositing as Au at the expense of Ag, which concomitantly oxidizes to Ag⁺ and is pushed into the sulfide domain. This is a reasonable hypothesis based on the similarities in the experimental details, including the reagents and the reaction conditions, between this exchange reaction and galvanic reactions that replace Ag with Au,²⁹ as well as literature precedent for metal cations to be exchanged between material domains in metal-semiconductor hybrid nanoparticles.³⁰ After the galvanic replacement reaction, Cu⁺ in AgCuS is replaced by Au⁺ to form AgAuS through a cation exchange process that occurs similarly to that involved in the transformation of Cu_{1.8}S to Au₂S.⁴ Lastly, additional Au, which is in excess at this stage of the reaction, deposits on the surface of the AgAuS particles.

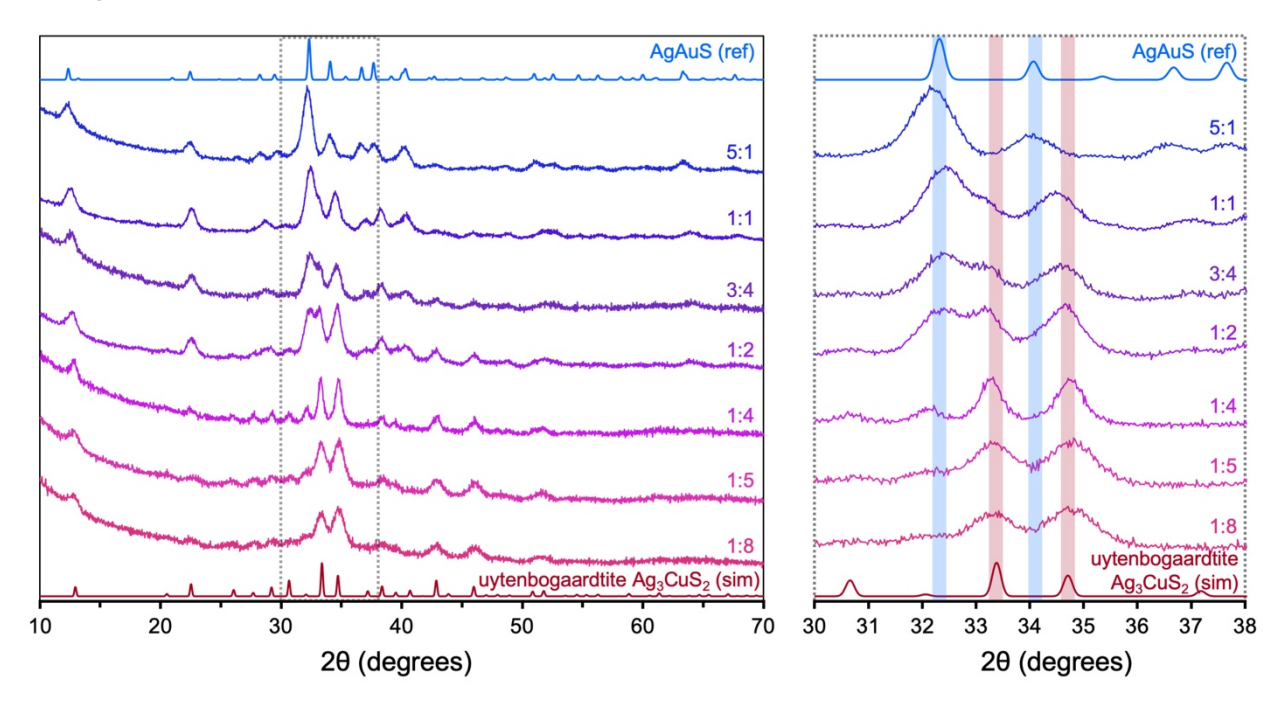


Figure 4. (a) Experimental XRD patterns corresponding to all Au:Cu exchange ratios with the uytenbogaardtite-type Ag₃CuS₂ simulated pattern on the bottom and the AgAuS reference pattern on the top. (b) Enlarged region of (a), denoted by the grey dotted box, highlighting the changes in the peak positions that are diagnostic of a transition from Ag₃CuS₂-type to AgAuS-type products.

XRD analysis provides additional insights into the reaction and how it proceeds. Figure 4 shows XRD patterns for all substoichiometric exchanges of Au⁺ for Cu⁺ (Au:Cu ratios of 1:8, 1:5, 1:4, 1:2, 3:4, 1:1, and 5:1) exchanges. As mentioned earlier, the final product matches well with AgAuS, which corresponds to the mineral petrovskaite. However, the intermediate XRD patterns require closer inspection to understand and rationalize the progression of this transformation.

The sample obtained from the lowest substoichiometric Au:Cu ratio (1:8), which represents the earliest stage of the reaction, produced an XRD pattern that does not match mckinstryite-type AgCuS, AgAuS, or other reported Ag-Cu-S phases. Rather, this sample qualitatively matches with an XRD pattern for Ag_3AuS_2 (PDF 01-080-9033), which corresponds to the mineral uytenbogaardtite, with peaks shifted to higher 20 and significant peak intensity differences. As

this experimental pattern corresponds to a sample generated from a substoichiometric exchange having insufficient Au, its composition cannot match that of uytenbogaardtite Ag_3AuS_2 . However, a simulated XRD pattern generated by replacing Au with Cu on all sites in uytenbogaardtite and empirically modifying the lattice parameters to match the experimental data does indeed match the experimental XRD pattern for the 1:8 sample. This change in lattice parameters reflects a decrease in unit cell volume of 2.82%, as would be expected upon replacing the larger Au^+ cation with the smaller Cu^+ cation to form uytenbogaardtite-type Ag_3CuS_2 .

We postulate that this structural transformation is initially induced by Ag⁺, which results from the galvanic replacement reaction, incorporating into the sulfide region. The uytenbogaardtite structure has a higher Ag content than mckinstryite and petrovskaite, which both have 3:1:2 vs 1:1:1 Ag:M:S (M = Au, Cu). The uytenbogaardtite-type Ag₃CuS₂ phase that appears in the 1:8 sample also accounts for all peaks in the experimental XRD patterns for the 1:5 and 1:4 samples. The only difference observed among these three XRD patterns is the peak narrowing at higher Au:Cu ratios, which we speculate can be accounted for by the progression of the galvanic replacement reaction leading to larger crystalline regions. However, as the Au:Cu ratio increases to and beyond 1:2, two phenomena occur. First, the uytenbogaardtite-type Ag₃CuS₂ XRD pattern begins to disappear while a different XRD pattern emerges. In the 1:2 pattern, this emerging XRD pattern corresponds to petrovskaite AgAuS, modified to have smaller lattice parameters that account for a decreased unit cell volume associated with substitution of Au⁺ for Cu⁺ to form AqAu₁₋ _xCu_xS. Second, there is a gradual shift of all peaks to lower 2θ values as the Au:Cu ratio increases, which indicates an increase in the lattice parameters of both crystalline components. These peak shifts are consistent with Cu-rich, Au-deficient uytenbogaardtite-type Ag₃Cu_xAu_{1-x}S₂ and petrovskaite-type AgCu_xAu_{1-x}S, as Au⁺ (137 pm) is significantly larger than Cu⁺ (60 pm).²⁹ Simulated XRD patterns containing a mixture of uytenbogaardtite-type Ag₃Cu_xAu_{1-x}S₂ and petrovskaite-type AgAu_{1-x}Cu_xS structures with appropriately modified lattice parameters and site occupancies match well with the experimental data for the 1:2 and 3:4 patterns (Figure S5), which supports our proposed transformation pathway.

The crystal structures of all starting, intermediate, and product sulfide phases, shown in Figure 5, also help us to understand how and why the transformations occur as they do. The progression of compounds elucidated from the studies described above suggest that the mckinstryite-type AgCuS transforms to uytenbogaardtite-type Ag₃CuS₂ (that becomes Ag₃Cu_xAu_{1-x}S₂ as more Au is added) and then to AgAuS. Ag₅Cu₃S₄ and Ag₃AuS₂ contain sulfur anions in a slightly distorted hexagonal close packed (hcp) arrangement with ABAB stacking of the close-packed sulfur layers. The anion structure of AgAuS is similar, but it cannot be described as hcp as it does not contain any close-packed planes. 30 All three compounds also contain metal-sulfur (M-S) layers, either Cu-S or Au-S, that sandwich layers of Au and/or Ag. In Ag₅Cu₃S₄, which is the starting structure type, the M-S layers have Cu⁺ mostly in trigonal planar coordination environments with S²⁻, along with a small amount having linear coordination. In AgAuS, which is the product phase, all Au⁺ is linearly coordinated with S^{2-} in the M-S layers. The chemical driving force for the reaction that ultimately transforms mckinstryite-type AgCuS to AgAuS is designed to selectively replace Cu⁺ with Au⁺. However, due to the significant difference in ionic radii between Cu⁺ (60 pm) and Au⁺ (137 pm),²⁹ structure retention during exchange is not favorable. The uytenbogaardtite intermediate serves as an Ag-rich, Au-poor structural framework that promotes site sharing between Ag and Au between the M-S layers and leaves space for Cu to remain in the M-S layers at low Au:Cu ratios. As the Au:Cu ratio increases, Au can start to incorporate into the M-S layers, coexisting and exchanging with Cu, and continue to site-share with Ag between the layers (as it does in the final AgAuS product). We hypothesize that the final transformation from the uytenbogaardtite-type structure to the petrovskaite-type structure occurs when the overall ratio of Au to Ag begins to approach 1:1, making the Au-poor uytenbogaardtite-type structure less favorable. Then, as the reaction reaches completion, the Cu is completely replaced by Au and all particles converge on petrovskaite AgAuS.

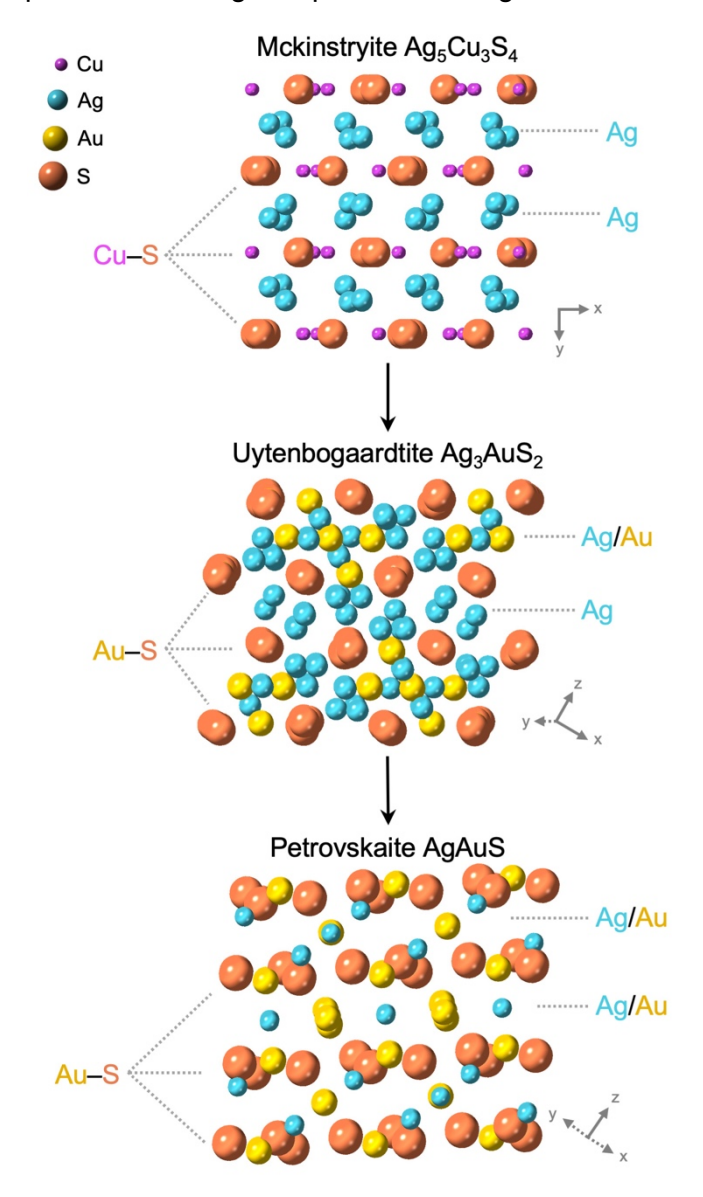


Figure 5. Comparison of the mckinstryite, uytenbogaardtite, and petrovskaite crystal structures, highlighting similarities and differences among them that help to rationalize an uytenbogaardtite-type structure that forms upon initial Au⁺ exchange of mckinstryite en route to the petrovskaite product.

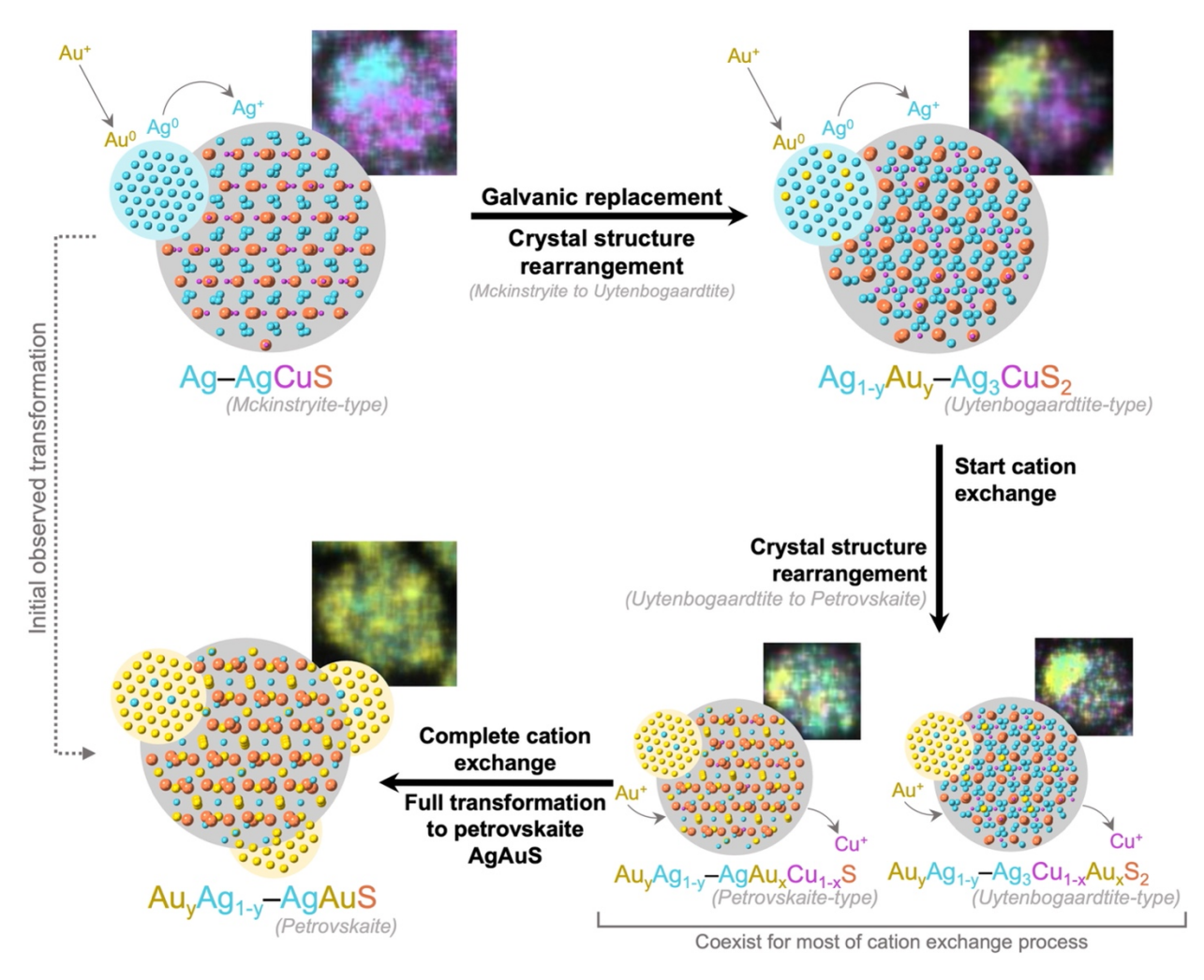


Figure 6. Overall proposed pathway for the transformation of mckinstryite-type AgCuS to petrovskaite AgAuS, as identified in this study.

CONCLUSIONS

In conclusion, we applied an established cation exchange reaction that replaces Cu⁺ with Au⁺ in copper sulfide nanoparticles^{3,4,19} to a mixed-metal sulfide, AgCuS, to understand the extent to which the chemical driving force for the Au⁺ exchange reaction was selective when two exchangeable monovalent cations, Cu⁺ and Ag⁺, were present. Rudimentary and high-level characterization suggested that AgCuS transformed to AgAuS as expected. However, a more comprehensive analysis, which applied STEM-EDS element mapping, XRD, and crystal structure relationships to aliquots taken as the reaction progressed, revealed a much more sophisticated multi-step pathway. The initial transformation proposed in Figure 1 is expanded in Figure 6 based on the data and analyses discussed above. As a brief summary, the as-synthesized AgCuS particles, which are better described as Ag–AgCuS where AgCuS is an off-stoichiometry variant of mckinstryite Ag₅Cu₃S₄, first undergo a galvanic replacement with Au⁺ to transform the Ag deposits to Au_yAg_{1-y}. This process is followed by transformation of the sulfide domain, mckinstryite-type AgCuS, to Ag₃Au_{1-x}Cu_xS₂ and then to AgAuS. The overall pathway can therefore

be described as Ag–AgCuS \rightarrow Au_yAg_{1-y}–Ag₃Cu_xAu_{1-x}S₂ \rightarrow Au_yAg_{1-y}–AgAuS. Beyond the detailed insights into the pathway, this study sheds light on the multi-step reactions that can occur during seemingly simple nanoparticle reactions as their compositional and structural complexity expands. Characterization beyond snapshots before and after the reaction, as well as more comprehensive analysis, is an important component of identifying and understanding such processes.

ASSOCIATED CONTENT

SUPPORTING INFORMATION

Additional STEM-EDS, XRD, and crystallographic data. This material is available free of charge via the Internet at http://pubs.acs.org.

AUTHOR INFORMATION

Corresponding Author

Raymond E. Schaak – Department of Chemistry, Department of Chemical Engineering, and Materials Research Institute, The Pennsylvania State University, University Park, Pennsylvania 16802, United States; Email: res20@psu.edu

Authors

Sarah K. O'Boyle – Department of Chemistry, The Pennsylvania State University, University Park, Pennsylvania 16802, United States

Katelyn J. Baumler – Department of Chemistry, The Pennsylvania State University, University Park, Pennsylvania 16802, United States

Notes

The authors declare no competing financial interest.

ACKNOWLEDGEMENT

This work was supported by the U.S. National Science Foundation under grant DMR-2210442. TEM and XRD data were acquired at the Materials Characterization Lab of the Penn State Materials Research Institute. The authors thank Gaurav Dey, Joseph Veglak, Katherine

Thompson, Connor McCormick,	Katherine Plass,	and Jennifer (Grey for helpful d	iscussions.

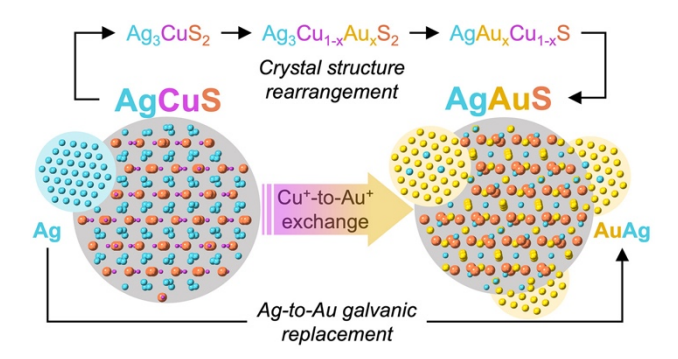
REFERENCES

- (1) Fenton, J. L.; Steimle, B. C.; Schaak, R. E. Tunable Intraparticle Frameworks for Creating Complex Heterostructured Nanoparticle Libraries. *Science* **2018**, *360* (6388).
- (2) Fenton, J. L.; Steimle, B. C.; Schaak, R. E. Structure-Selective Synthesis of Wurtzite and Zincblende ZnS, CdS, and CulnS₂ Using Nanoparticle Cation Exchange Reactions. *Inorg. Chem.* **2019**, *58* (1), 672–678.
- (3) Park, J.; Park, J.; Lee, J.; Oh, A.; Baik, H.; Lee, K. Janus Nanoparticle Structural Motif Control via Asymmetric Cation Exchange in Edge-Protected Cu_{1.81}S@Ir_xS_y Hexagonal Nanoplates. *ACS Nano* **2018**, *12* (8), 7996–8005.
- (4) Hernández-Pagán, E. A.; O'Hara, A.; Arrowood, S. L.; McBride, J. R.; Rhodes, J. M.; Pantelides, S. T.; Macdonald, J. E. Transformation of the Anion Sublattice in the Cation-Exchange Synthesis of Au₂S from Cu_{2-x}S Nanocrystals. *Chem. Mater.* **2018**, *30* (24), 8843–8851.
- (5) Steimle, B. C.; Fenton, J. L.; Schaak, R. E. Rational Construction of a Scalable Heterostructured Nanorod Megalibrary. *Science* **2020**, *367* (6476), 418–424.
- (6) Gan, X. Y.; Sen, R.; Millstone, J. E. Connecting Cation Exchange and Metal Deposition Outcomes via Hume–Rothery-Like Design Rules Using Copper Selenide Nanoparticles. *J. Am. Chem. Soc.* **2021**, *143* (21), 8137–8144.
- (7) Li, Z.; Saruyama, M.; Asaka, T.; Tatetsu, Y.; Teranishi, T. Determinants of Crystal Structure Transformation of Ionic Nanocrystals in Cation Exchange Reactions. *Science* **2021**, 373 (6552), 332–337. https://doi.org/10.1126/science.abh2741.
- (8) Ha, D.-H.; Caldwell, A. H.; Ward, M. J.; Honrao, S.; Mathew, K.; Hovden, R.; Koker, M. K. A.; Muller, D. A.; Hennig, R. G.; Robinson, R. D. Solid–Solid Phase Transformations Induced through Cation Exchange and Strain in 2D Heterostructured Copper Sulfide Nanocrystals. *Nano Lett.* 2014, 14 (12), 7090–7099.
- (9) Son, D. H.; Hughes, S. M.; Yin, Y.; Paul Alivisatos, A. Cation Exchange Reactions in Ionic Nanocrystals. *Science* **2004**, *306* (5698), 1009–1012.
- (10) Kim, T.; Park, J.; Hong, Y.; Oh, A.; Baik, H.; Lee, K. Janus to Core–Shell to Janus: Facile Cation Movement in Cu_{2-x}S/Ag₂S Hexagonal Nanoplates Induced by Surface Strain Control. *ACS Nano* **2019**, *13* (10), 11834–11842.
- (11) Steimle, B. C.; Fagan, A. M.; Butterfield, A. G.; Lord, R. W.; McCormick, C. R.; Di Domizio, G. A.; Schaak, R. E. Experimental Insights into Partial Cation Exchange Reactions for Synthesizing Heterostructured Metal Sulfide Nanocrystals. *Chem. Mater.* **2020**, *32* (13), 5461–5482.
- (12) Enright, M. J.; Cossairt, B. M. Synthesis of Tailor-Made Colloidal Semiconductor Heterostructures. *Chem. Commun.* **2018**, *54* (52), 7109–7122.
- (13) Sadtler, B.; Demchenko, D. O.; Zheng, H.; Hughes, S. M.; Merkle, M. G.; Dahmen, U.; Wang, L.-W.; Alivisatos, A. P. Selective Facet Reactivity during Cation Exchange in Cadmium Sulfide Nanorods. *J. Am. Chem. Soc.* **2009**, *131* (14), 5285–5293.

- (14) Robinson, R. D.; Sadtler, B.; Demchenko, D. O.; Erdonmez, C. K.; Wang, L.-W.; Alivisatos, A. P. Spontaneous Superlattice Formation in Nanorods Through Partial Cation Exchange. *Science* **2007**, *317* (5836), 355–358.
- (15) O'Boyle, S. K.; Fagan, A. M.; Steimle, B. C.; Schaak, R. E. Expanded Tunability of Intraparticle Frameworks in Spherical Heterostructured Nanoparticles through Substoichiometric Partial Cation Exchange. *ACS Mater. Au* **2022**, *2* (6), 690–698.
- van der Stam, W.; Berends, A. C.; Rabouw, F. T.; Willhammar, T.; Ke, X.; Meeldijk, J. D.; Bals, S.; de Mello Donega, C. Luminescent CuInS₂ Quantum Dots by Partial Cation Exchange in Cu_{2-x}S Nanocrystals. *Chem. Mater.* 2015, 27 (2), 621–628.
- (17) Fenton, J. L.; Steimle, B. C.; Schaak, R. E. Exploiting Crystallographic Regioselectivity To Engineer Asymmetric Three-Component Colloidal Nanoparticle Isomers Using Partial Cation Exchange Reactions. *J. Am. Chem. Soc.* **2018**, *140* (22), 6771–6775.
- (18) Fagan, A. M.; Steimle, B. C.; Schaak, R. E. Orthogonal Reactivity and Interface-Driven Selectivity during Cation Exchange of Heterostructured Metal Sulfide Nanorods. *Chem. Commun.* **2022**, *58* (27), 4328–4331.
- (19) Dalmases, M.; Torruella, P.; Blanco-Portals, J.; Vidal, A.; Lopez-Haro, M.; Calvino, J. J.; Estradé, S.; Peiró, F.; Figuerola, A. Gradual Transformation of Ag₂S to Au₂S Nanoparticles by Sequential Cation Exchange Reactions: Binary, Ternary, and Hybrid Compositions. *Chem. Mater.* **2018**, *30* (19), 6893–6902.
- (20) Sahu, P.; Prusty, G.; Guria, A. K.; Pradhan, N. Modulated Triple-Material Nano-Heterostructures: Where Gold Influenced the Chemical Activity of Silver in Nanocrystals. *Small* **2018**, *14* (33), 1801598.
- (21) Kuzuya, T.; Kuwada, T.; Inukai, H.; Hamanaka, Y.; Hirai, S. Synthesis of Ag/AgCuS/CuInS₂ Hybrid Nanoparticles by Reductive Cation Exchange and Their Asymmetric Heterostructure. *Appl. Surf. Sci.* **2019**, *493*, 1278–1285.
- (22) Sato, K.; Kuzuya, T.; Hamanaka, Y.; Hirai, S. Synthesis and Analysis of Highly Monodispersed Silver Copper Sulfide Nanoparticles. *Mater. Trans.* **2021**, *62* (6), 731–737.
- (23) Pradyasti, A.; Kim, D. S.; Kim, M. H. Synthesis of Au@AgAuS Core—Shell Hybrid Nanorods and Their Photocatalytic Application. *Colloids Interface Sci. Commun.* **2022**, *49*, 100635.
- (24) Li, X.; Schaak, R. E. Reactive AgAuS and Ag₃AuS₂ Synthons Enable the Sequential Transformation of Spherical Nanocrystals into Asymmetric Multicomponent Hybrid Nanoparticles. *Chem. Mater.* **2017**, 29 (9), 4153–4160.
- (25) Trolier-Mckinstry, S.; Newnham, R. E. *Materials Engineering: Bonding, Structure, and Structure-Property Relationships*; Cambridge University Press: Cambridge, United Kingdom, 2018.
- (26) de Graaf, P. W. J.; Boersma, J.; van der Kerk, G. J. M. Preparation and Properties of Arylgold Compounds. Scope and Limitations of the Auration Reaction. *J. Organomet. Chem.* **1976**, *105* (3), 399–406.

- (27) Kolitsch, U. The Crystal Structure and Compositional Range of Mckinstryite. *Mineral. Mag.* **2010**, *74* (1), 73–84.
- (28) Lide, D. R. CRC Handbook of Chemistry and Physics, 85th Edition; CRC Press, 2004.
- (29) Polavarapu, L.; M. Liz-Marzán, L. Growth and Galvanic Replacement of Silver Nanocubes in Organic Media. *Nanoscale* **2013**, *5* (10), 4355–4361.
- (30) Lin, M.; Montana, G.; Blanco, J.; Yedra, L.; van Gog, H.; van Huis, M. A.; López-Haro, M.; Calvino, J. J.; Estradé, S.; Peiró, F.; Figuerola, A. Spontaneous Hetero-Attachment of Single-Component Colloidal Precursors for the Synthesis of Asymmetric Au–Ag₂X (X = S, Se) Heterodimers. *Chem. Mater.* **2022**.

Table of Contents Graphic



Synposis: Attempts at exchanging the Cu⁺ cations in AgCuS nanoparticles with Au⁺ to form AgAuS did not proceed as expected, but rather through a multi-reaction pathway involving galvanic replacement, cation exchange, and metal deposition, as well as formation of a structural intermediate that crystallographically relates the AgCuS precursor and AgAuS product.